International Journal of Mechanical, Industrial and Aerospace Sciences
ISSN: 2517-9950
Vol:13, No:6, 2019

Power Efficiency Characteristics of Magnetohydrodynamic Thermodynamic Gas Cycle

Mahmoud Huleihil

***Abstract*—**In this study, the performance of a thermodynamic gas cycle of magnetohydrodynamic (MHD) power generation is considered and presented in terms of power efficiency curves. The dissipation mechanisms considered include: fluid friction modeled by means of the isentropic efficiency of the compressor, heat transfer leakage directly from the hot reservoir to the cold heat reservoir, and constant velocity of the MHD generator. The study demonstrates that power and efficiency vanish at the extremes of both slow and fast operating conditions. These points are demonstrated on power efficiency curves and the locus of efficiency at maximum power and the locus of maximum efficiency. Qualitatively, the considered loss mechanisms have a similar effect on the efficiency at maximum power operation and on maximum efficiency operation, thus these efficiencies are reduced, even for small values of the loss mechanisms.

***Keywords*—**magnetohydrodynamic generator, electrical efficiency, maximum power, maximum efficiency, heat engine.

I. Introduction

MHD generation is based on Faraday's law of electromagnetic induction, with the working fluid in this device being a plasma-ionized gas [1]. In principle, the MHD generator is a variation of the Faraday generator, in which Faraday's solid conductors are replaced by a moving electricity conducting fluid, and the electricity is produced directly [2]. Research and development programs that focused on open cycle, closed cycle plasma, and liquid metal MHD are described in [3]. The MHD generator appears to have wide applicability and its development is progressing both rapidly and encouragingly [4]. A theoretical model to analyze the performance characteristics of an MHD generator power plant is presented in [5]. MHD power generation technology offers an attractive generation potential to the electric utilities [6]. A short history, MHD types, basic concepts, and theory are described in [7].

In this study, MHD power generation is reconsidered in order to account for different types of irreversibility. The MHD power cycle is approximated by the Brayton cycle, with irreversibility types including fluid friction in the compressor, which is modeled by means of the compressor's isentropic efficiency, heat leakage from the hot side to the cold side of the heat engine, and the constant working speed of the working fluid crossing the MHD generator. The performance characteristics of the MHD system are presented in terms of power-efficiency curves as were those performed in [8], [9].

In Section II, the basic principles of the MHD generator are reviewed; in Section III, the different irreversibility mechanisms are considered, in Section IV, power and efficiency curves are presented as well as maximum power operation and maximum efficiency operation for various numerical values of dissipation parameters, and in Section V, a discussion is given; and finally, in Section VI, the summary and conclusions are presented.

Mahmoud Huleihil is with The Arab Academic Institute of Education, Beit-Berl College, Kfar Saba 44905, Israel (phone: +972-52-7871099, fax: +972-9-4746213, e-mail: mahmud.ana@gmail.com).

II. Basic MHD Power Generation Cycle

The principles behind MHD power generation [1]-[7] are simple and have been known since 1831. However, the engineering necessary to generate electricity cheaply by MHD is complex. As mentioned earlier, the MHD generator is a variation of the Faraday generator, in which the solid conductors are replaced by a moving electrically conducting working fluid. Classically, electrical power is produced by burning fuel. The conversion is usually performed by combusting a chemical compound or fossil fuel with an oxidizer which is usually oxygen. The result of this combustion process is expressed by transferring the stored chemical energy of the fuel into thermal energy, which is now contained in the products of the combustion. Then, the produced thermal energy is usually converted directly into mechanical energy by different ways, such as an internal combustion engine or an external combustion engine such as a gas turbine. The conversion can also take place indirectly by transferring the thermal energy into a different working fluid via heat exchangers, from which mechanical power could be extracted in a closed thermodynamic cycle, such as a gas or steam cycle. In the case of a nuclear power plant, the energy is normally converted into thermal energy in the fuel rods, which is then transferred into a coolant, and afterwards is converted into mechanical energy. Eventually, the mechanical energy is converted into electrical energy by means of a generator (dynamo). If the working fluid in either case—combustion gases or nuclear power plant coolant—could be made electrically conducting and could have been converted into a directed flow such that some part of its thermal energy is converted into kinetic energy. Then, the working fluid could be passed directly into a magnetic field. By doing that, the kinetic energy is converted directly into electrical energy, thus eliminating the mechanical intermediary steps.

There are three types of MHD power generation systems: open cycle (the hot gases are exhausted to the atmosphere), closed cycle plasma (heat transfer occurs by means of heat exchangers), and liquid metal. In a coal-fired open-cycle

MHD power plant (see Fig. 1), coal is burned in a combustion chamber with a working fluid including a seed material, e.g. potassium carbonate, K_2CO_3. The rule of the seed material is to enhance the electrically charged working fluid temperatures (see Fig. 2). This electrically charged gas escapes from the combustion chamber through a nozzle, thus producing a high velocity stream of particles that are both positively and negatively charged. These negatively and positively particles, while passing between the coils of powerful electromagnets, move in opposite directions and collide with two different electrical collector plates (one of which becomes the positive, and the other the negative – see Fig. 2), thus enabling the electrical terminal of the MHD generator. The direct electrical current produced is then converted to an alternating current in order to be compatible with current utility systems [2].

There are many advantages to using MHD generation of electricity, when compared to the usual methods of power generation that use steam or gas turbines. These include the benefits of avoiding moving parts (no mechanical friction) as well as exposing them to high temperatures, thus eliminating steam corrosion of the turbine blades.

The potential advantage of MHD power generation is based on utilizing the higher temperatures of the working fluid, rather than being limited to fluids that are compatible with turbines. This may lead to either higher overall thermal efficiencies, or in the case of "space power," to a higher reject temperature and thus a reduction of the radiator area [2].

Nuclear reactions and geothermal sources and concentrated solar radiation are potential sources to MHD generators. However, heat coming from coal combustion gases was as the heat source in the United States [2], [7].

The schematics of MHD power generation system are depicted in Fig. 1.

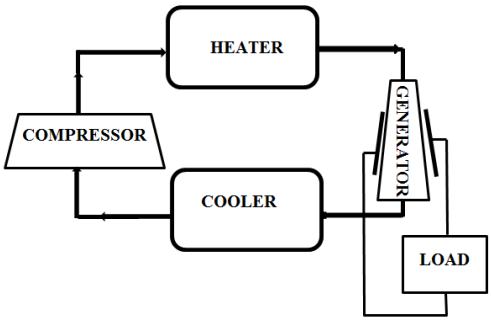

Fig. 1 Schematics of an MHD power generation system

The components are similar in concept and function to a gas turbine system, except that the turbine component is replaced by an MHD generator (see Fig. 2). The ideal compressor is modeled as an isentropic process and its real behavior is modeled via the isentropic efficiency, which is described in section III. Heat addition and rejection are performed in the heater and cooler, respectively. The MHD power generator is modeled as high constant velocity unit [5].

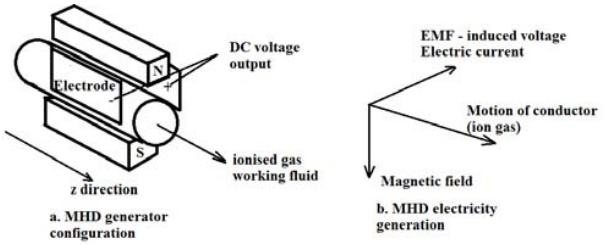

Fig. 2 Schematics of MHD generator. In part a, the ionized gas crosses the magnet at high velocity, thus producing electrical current, as depicted in part b

III. Irreversibility Mechanisms

In this study, the MHD system is modeled on the gas turbine thermodynamic cycle from the ideal Brayton cycle, with certain shifts, which are considered and modeled as non-isentropic process in the compression process. These shifts focus on the constant speed MHD generator (shifts from isentropic turbine) and heat leak.

MHD Generator Model

Consider an MHD power generation unit with compressible ideal gas working fluid that is operating with constant specific heat. The unit cycle includes the following processes: an irreversible compressor with isentropic efficiency η_c; constant pressure heat addition; an MHD generator with constant velocity; constant pressure heat rejection (see Fig. 3).

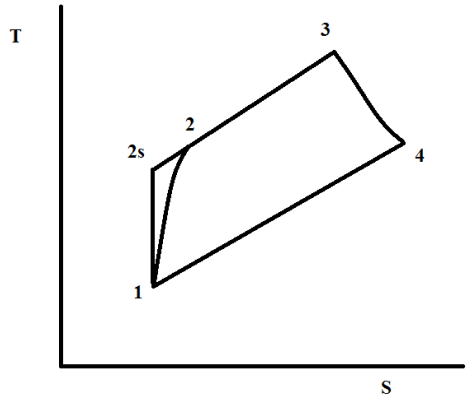

Fig. 3 Temperature vs. entropy [T-S] diagram of Bayton-MHD thermodynamic cycle

The T-S diagram includes the following processes: 1-2 realistic compression process, 2-3 constant pressure heat addition, 3-4 constant velocity expansion (MHD generator), and 4-1 constant heat rejection and thus completing the cycle.

One-Dimensional MHD Model

For one-dimensional steady state flow, the conservation of momentum and energy for the MHD generator is given respectively, as follows [10]:

Momentum conservation:

$$\rho u\frac{du}{dz}+\frac{dp}{dz}+JB=0 \quad (1)$$

where ρ is the density of the working fluid, u is the velocity of the working fluid, p is the pressure of the working fluid, J is the current density, B is the magnetic field, and E is the electric field.

Energy Conservation:

$$\rho u\frac{d(h+½u^2)}{dz}+JE=0 \quad (2)$$

where h is the working fluid enthalpy.

The ionized working fluid properties are derived from the ideal gas equation of state and are given by:

$$p=\rho RT \quad (3)$$

where R is the ideal gas constant and T is the temperature of the working fluid.

The change of enthalpy for ideal gas with constant specific heat c_p is given by:

$$dh=c_p dT \quad (4)$$

The electrical efficiency of the MHD generator is defined as [5], [10]:

$$\eta_e=\frac{JE}{uJB} \quad (5)$$

Using (1)-(5) will dictate a corresponding state at the exit of the MHD generator.

Constant Velocity Condition

In the case of constant velocity, the working fluid (ideally gas), in the generator does not decelerate. The electrical current and thus the electrical power comes from the work done by the expansion of the gas against the magnetic forces, i.e. from the energy transmission— the enthalpy or thermal energy of the working fluid.

By manipulating the model with (1)-(5), the state at the exit of the MHD generator is determined and is given by:

Momentum conservation:

$$\frac{dp}{dz}=-JB \quad (6)$$

Energy conservation:

$$\rho c_p\frac{dT}{dz}=-\frac{JE}{u} \quad (7)$$

By further manipulating (3), and (5)-(7), the relation between pressure and temperature of the working fluid at the exit of the MHD generator is given by:

$$\frac{T}{P^{\frac{k-1}{k}\eta_e}}=const. \quad (8)$$

Heat addition to the power unit: The application of the first law of thermodynamics from state 2 to state 3 will dictate the amount of heat input to the power unit and is given by:

$$Q_H=c_p\left(T_3-T_2\right) \quad (9)$$

Heat rejection from the power unit: Similarly, the application of the first law of thermodynamics from state 4 to state 1 will dictate the amount of energy rejected from the power unit and is given by:

$$Q_L=c_p\left(T_4-T_1\right) \quad (10)$$

The ideal process across the compressor is isentropic, and the actual process is defined by using the isentropic efficiency η_c which is given by:

$$\eta_c=\frac{T_{2s}-T_1}{T_2-T_1} \quad (11)$$

Finally, the temperature at the exit of the MHD generator T4 is given by:

$$T_4=\frac{T_3}{a^{\eta_e}} \quad (12)$$

where a is defined by:

$$a=\left(\frac{p_3}{p_1}\right)^{\frac{k-1}{k}} \quad (13)$$

After using relations (9), (11), (12), the heat addition to the power unit could be formulated by:

$$Q_H=c_pT_3\left(1-\frac{\tau a}{\eta_c}+\tau\left(\frac{1}{\eta_c}-1\right)\right) \quad (14)$$

where τ is the ratio between the minimal temperature and the maximal temperature, i.e. T_1/T_3.

After using (10)-(12), the heat rejection from the power unit could be formulated by:

$$Q_L=c_pT_3\left(\frac{1}{a^{\eta_e}}-\tau\right) \quad (15)$$

The network output w_{net} of the power unit is given by:

$$w_{net} = Q_H - Q_L = c_p T_3 \left(1 - \frac{\tau a}{\eta_c} + \frac{\tau}{\eta_c} - \frac{1}{a^{\eta_e}}\right) \quad (16)$$

Finally, the thermal efficiency η of the power unit is given by:

$$\eta = \frac{w_{net}}{Q_H} \quad (17)$$

Effect of heat leak

For currently functioning power units there always will be heat transfer to the environment. This heat leakage, unfortunately, does not contribute to power generation. In this study, heat leakage is modeled as proportional to the difference between the maximal and minimal temperatures, with proportionality constant k_{Leak} (see Fig. 4).

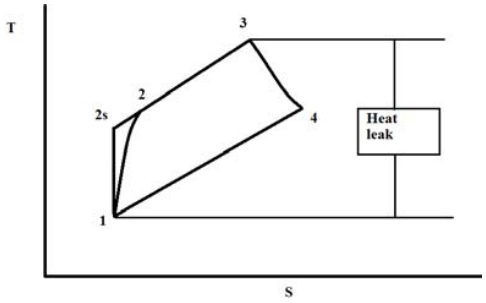

Fig. 4 T-S diagram of Bayton-MHD thermodynamic cycle with heat leak

The T-S diagram is similar to Fig. 3, with the addition of the heat leak process shown as 3-1, in which heat transfer is lost without actually producing useful power. The source of this loss is due to the realistic behavior of the materials used; the processes are not hermetically adiabatic.

The heat leak transfer is given by:

$$Q_{Leak} = k_{Leak}\left(T_3 - T_1\right) \quad (18)$$

This amount of heat leakage is added to the heat transfer rates entering and exiting from the power unit. Equations (9) and (10) are modified accordingly and the heat addition Q_{input} and heat rejection Q_{output} are respectively given by:

$$Q_{input} = Q_H + Q_{Leak} \quad (19)$$

$$Q_{output} = Q_L + Q_{Leak} \quad (20)$$

As can be seen from the difference between (20) and (19), the network output is not changed and (16) holds, but the efficiency expression is modified and is given by:

$$\eta = \frac{w_{net}}{Q_{input}} \quad (21)$$

The aforementioned relations of net power output and thermal efficiency could be derived with respect to parameter a in order to reach maximal power output and maximal efficiency. The conditions for optimality are respectively given by:

$$\frac{dw_{net}}{da} = 0; \quad (22)$$

and

$$\frac{d\eta}{da} = 0; \quad (23)$$

It is worth noting that all three irreversibility conditions lead to maximal efficiency point separately, while in the ideal case the maximal efficiency is limited by the Carnot efficiency, which is given by:

$$\eta_{Carnot} = 1 - \frac{T_1}{T_3}; \quad (24)$$

For convenience and for producing power-efficiency plots, the non-dimensional power p^* is defined as the ratio between $\frac{w}{c_p T_3}$ and its maximum value $\left(1-\sqrt{\tau}\right)^2$ and is given by:

$$p^* = \frac{\left(1 - \frac{\tau a}{\eta_c} + \frac{\tau}{\eta_c} - \frac{1}{a^{\eta_e}}\right)}{\left(1-\sqrt{\tau}\right)^2} \quad (25)$$

For efficiency calculations the dimensionless heat leak parameter is given by:

$$k^*_{leak} = \frac{k_{leak}}{c_p} \quad (26)$$

The maximum power point was achieved by means of (22). By differentiating (16) with respect to the parameter and equating to zero, the value of the parameter *a* could be derived at this point, and is given by:

$$a = \left(\frac{\eta_e}{\tau \eta_c}\right)^{\frac{1}{1+\eta_e}} \quad (27)$$

Finally, the maximum efficiency point could be achieved by means of (23). By differentiating (21) and equating to zero, the value of parameter *a* could be derived at this point, and its numerical value could be calculated numerically. The

Microsoft Excel GOALSEEK tool was used to find the maximum efficiency point.

IV. Numerical Examples

In this section, the power-efficiency curves, maximum power point, and maximum efficiency are considered numerically. Equation (21) is used for efficiency calculations, and (25) is used for power production calculation. Equation (27) supplies the value of the variable a at maximum power operation. For each possibility, four cases are considered: effect of electrical efficiency, effect of isentropic efficiency, effect of constant velocity of the working fluid in the MHD generator, and the combined effect of all three mechanisms. The numerical values of the four different cases are as follows:

Effect of electrical efficiency:

For each electrical efficiency considered, the other parameters are fixed at the specified value.

$$\eta_e = 0.85, 0.9, 0.95, 1.0$$
$$\eta_c = 1.0$$
$$k^*_{leak} = 0$$

Effect of isentropic efficiency:

For each isentropic efficiency considered, the other parameters are fixed at the specified value.

$$\eta_e = 1.0$$
$$\eta_c = 0.85, 0.9, 0.95, 1.0$$
$$k^*_{leak} = 0$$

Effect of dimensionless heat leak parameter:

For each dimensionless heat leak parameter considered, the other parameters are fixed at the specified value.

$$\eta_e = 1.0$$
$$\eta_c = 1.0$$
$$k^*_{leak} = 0.15, 0.1, 0.05, 0.0$$

Combined effect of all dissipation mechanisms:

The values of the parameters change towards the ideal case and are taken one column at a time (matrix 3x4).

$$\eta_e = 0.85, 0.9, 0.95, 1.0$$
$$\eta_c = 0.85, 0.9, 0.95, 1.0$$
$$k^*_{leak} = 0.15, 0.1, 0.05, 0.0$$

A. Power Efficiency Characteristics

The characteristics of the heat engine are presented in terms of power-efficiency plots (see Figs. 5-8). These plots were produced by means of (25). The locus of the maximum power points was added to the plots by means of (27), and the maximum efficiency locus was added to the plots by means of the GOALSEEK tool of Microsoft Excel.

1. Effect of the Electrical Efficiency

The following values were used for electrical efficiency—1.0, 0.95, 0.9, and 0.85.

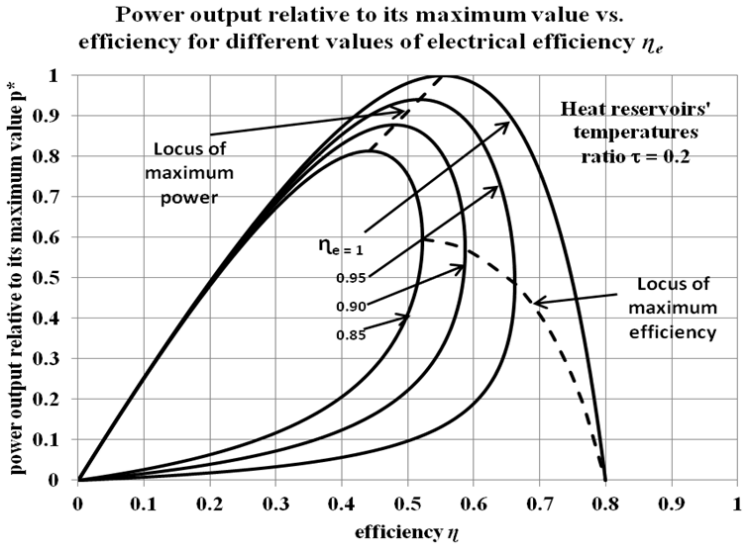

Fig. 5 The effect of electrical efficiency on the power – efficiency curve

As can be seen from Fig. 5, the power and the efficiency are concentrated at the extremes, for both slow and fast operations. In the theoretically ideal case, the electrical efficiency is 1.0, the isentropic efficiency is 1.0, and the heat leak parameter is zero. The maximum efficiency point is reduced when the electrical efficiency is reduced and its value approaches the maximum power point (see locus of maximum power point and maximum efficiency point).

2. Effect of the Isentropic Efficiency

The following values were used for the isentropic efficiency – 1.0, 0.95, 0.9, and 0.85.

As can be seen from Fig. 6, the power and efficiency are concentrated at the extremes, for both slow and fast operations. In the theoretically ideal case, the isentropic efficiency is 1.0, the electrical efficiency is 1.0 and the heat leak parameter is zero. The maximum efficiency point is reduced when the isentropic efficiency is reduced and its value approaches the maximum power point (see locus of maximum power point and maximum efficiency point).

3. Effect of Heat Leak

The following values were used for the dimensionless heat leak parameter —0.0, 0.05, 0.1, and 0.15.

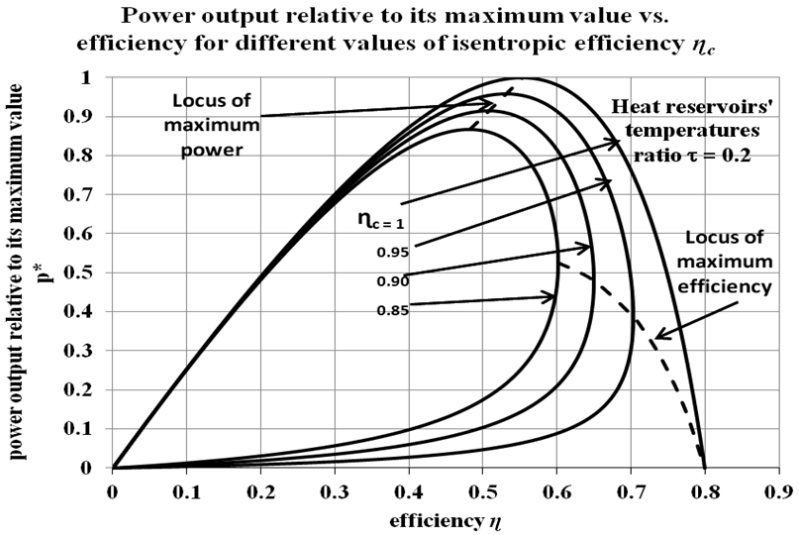

Fig. 6 The effect of the isentropic efficiency on the power – efficiency curve

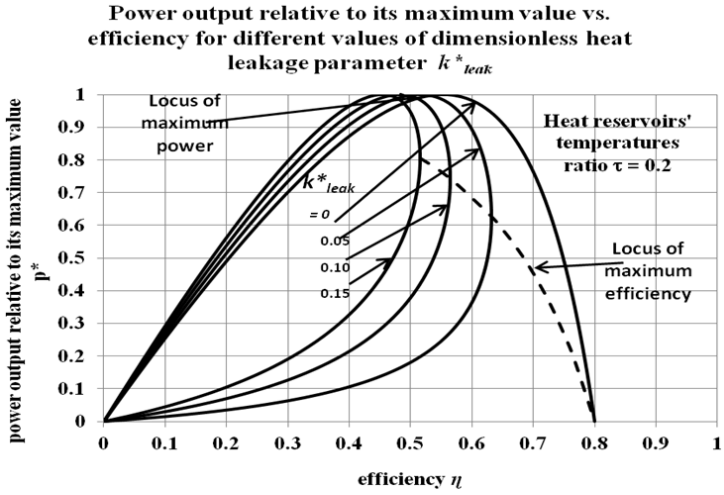

Fig. 7 The effect of the dimensionless heat leak parameter on the power – efficiency curve

As can be seen from Fig. 7, the power and efficiency are concentrated at the extremes, for both slow and fast operations. In the theoretically ideal case, the dimensionless heat leak parameter is 0.0, the electrical efficiency is 1.0, and the isentropic efficiency is 1.0. The maximum efficiency point is reduced when the dimensionless heat leak parameter is increased and its value approaches the maximum power point (see locus of maximum power point and maximum efficiency point).

4. Combined Effect of the Dissipation Mechanisms

The following values of the dissipation parameters were used as was described in the numerical section. Three value sequences were used for dissipation as follows: 1.0, 1.0, 0.0 for ideal case; the values are given for electrical efficiency and isentropic efficiency and dimensionless heat leakage coefficient in order. The other sequence values are: 0.95, 0.95, 0.05; 0.9, 0.9, 1.0; and 0.85, 0.85, 0.15. 9 were used;

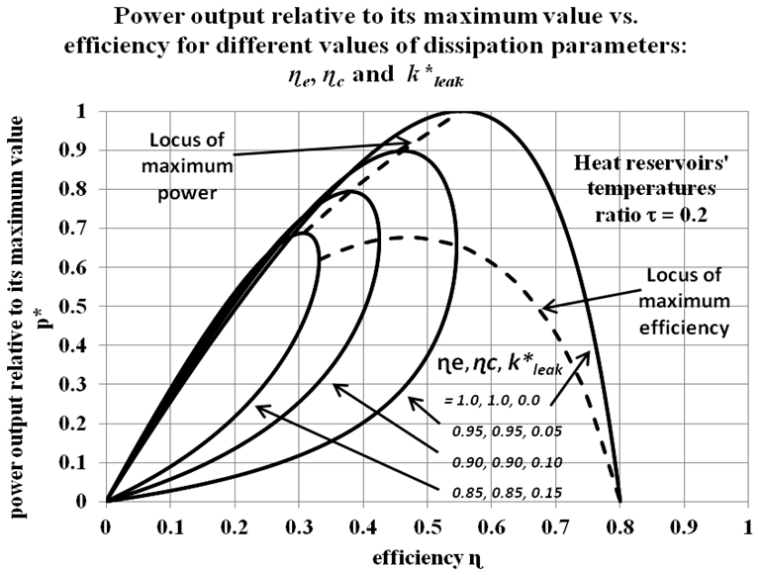

Fig. 8 The combined effect of all dissipation mechanisms c on the power – efficiency curve

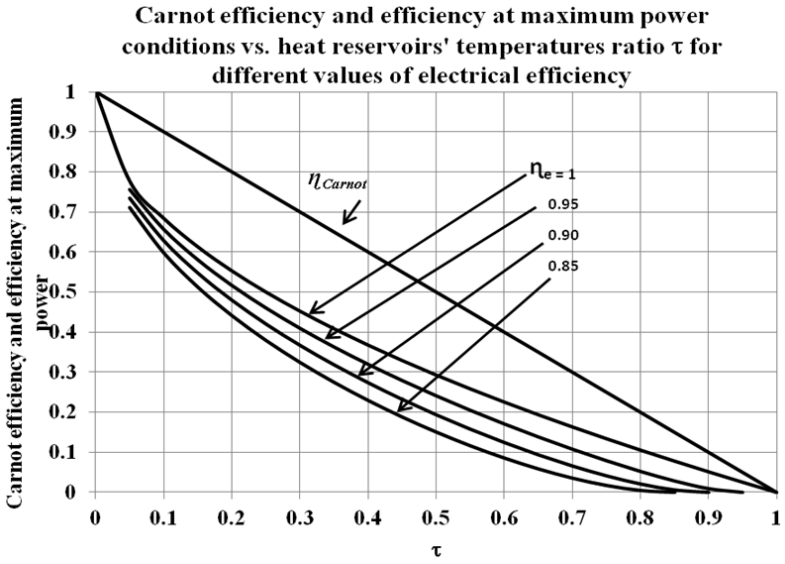

Fig. 9 Efficiency at the maximum power point plotted as a function of the variable τ and the electrical efficiency parameter

As can be seen from Fig. 8, the power and efficiency are concentrated at the extremes, for both slow and fast operations. In the theoretically ideal case, the dimensionless heat leak parameter is 0.0, the electrical efficiency is 1.0, and the isentropic efficiency is 1.0. The maximum efficiency point is reduced when the dimensionless heat leak parameter is increased and the electrical efficiency and the isentropic efficiency are increased and its value approaches the maximum power point (see locus of maximum power point and maximum efficiency point).

B. Maximum Power Point Operation

Equation (27) was used to dictate the value of the maximum power point as a function of the variable τ . Four cases were used, as was described in the numerical examples section.

1. Effect of Electrical Efficiency

The following values were used for electrical efficiency—1.0, 0.95, 0.9, and 0.85.

As can be seen from Fig. 9, the maximum power point is reduced below the case of electrical efficiency of value 1.0.

2. Effect of the Isentropic Efficiency

The following values were used for the isentropic efficiency —1.0, 0.95, 0.9, and 0.85.

As can be seen from Fig. 10, the maximum power point is reduced below the case of isentropic efficiency of value 1.0.

3. Effect of Heat Leak

The following values were used for the dimensionless heat leak parameter —0.0, 0.05, 0.1, and 0.15.

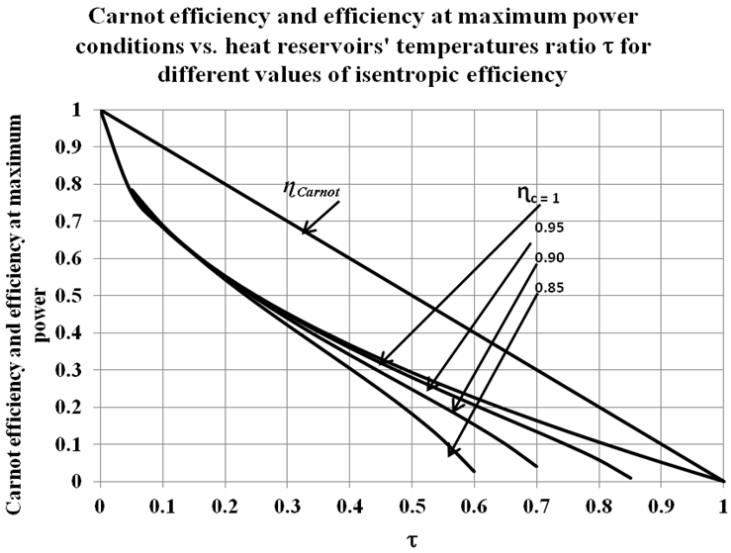

Fig. 10 Efficiency at maximum power point plotted as a function of the variable τ and the isentropic efficiency parameter

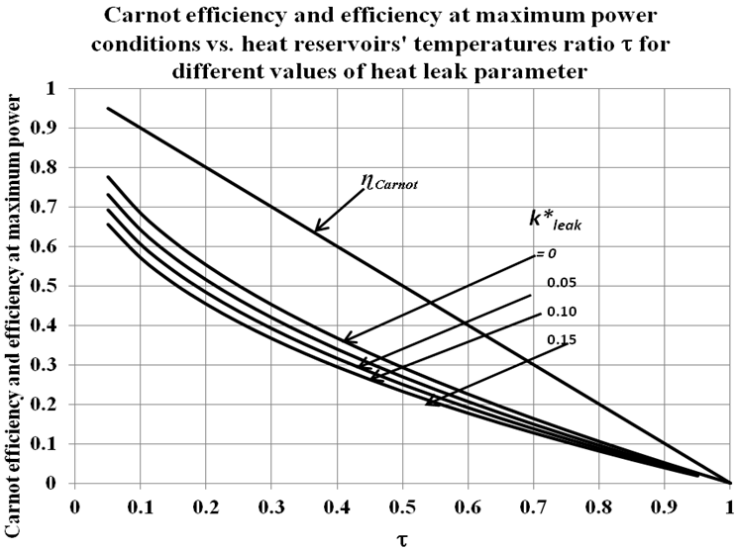

Fig. 11 The efficiency at maximum power point plotted as a function of the variable τ and the dimensionless heat leak parameter

As can be seen from Fig. 11, the maximum power point is reduced below the case of zero dimensionless heat leak parameter.

4. Combined Effect of the Dissipation Mechanisms

The following values of the dissipation parameters were used as was described in the numerical section. Three value sequences were used for dissipation as follows: 1.0, 1.0, 0.0 for ideal case; the values are given for electrical efficiency and isentropic efficiency and dimensionless heat leakage coefficient in order. The other sequence values are: 0.95, 0.95, 0.05; 0.9, 0.9, 1.0; and 0.85, 0.85, 0.15. 9 were used.

As can be seen from Fig. 12, the maximum power point is reduced below the case of zero dimensionless heat leak parameter, electrical efficiency of value 1.0, and isentropic efficiency of 1.0.

C. Maximum Efficiency Conditions

Equation (21) was used to find the maximum efficiency point by means of the GOALSEEK tool of the Microsoft Excel program. Four values of dissipation parameters were used, as were described in the numerical examples sections.

1. Effect of Electrical Efficiency

The following values were used for electrical efficiency—1.0, 0.95, 0.9, and 0.85.

As can be seen from Fig. 13, the maximum efficiency point is reduced below the case of Carnot efficiency.

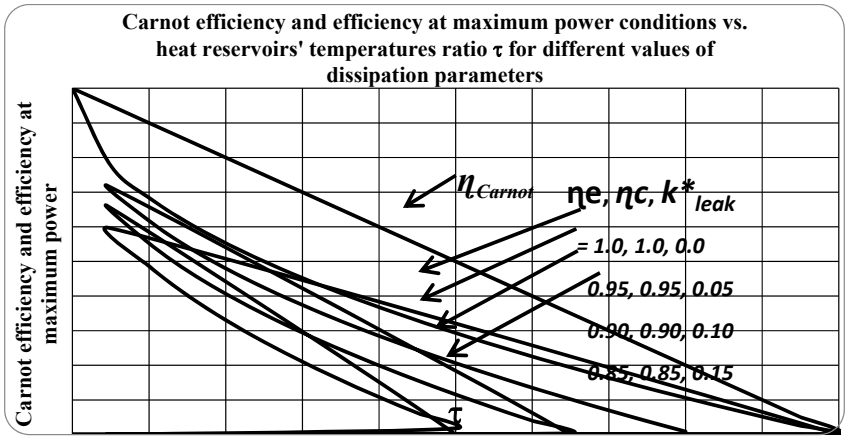

Fig. 12 Efficiency at maximum power point plotted as a function of the variable τ and the combined dissipation parameters

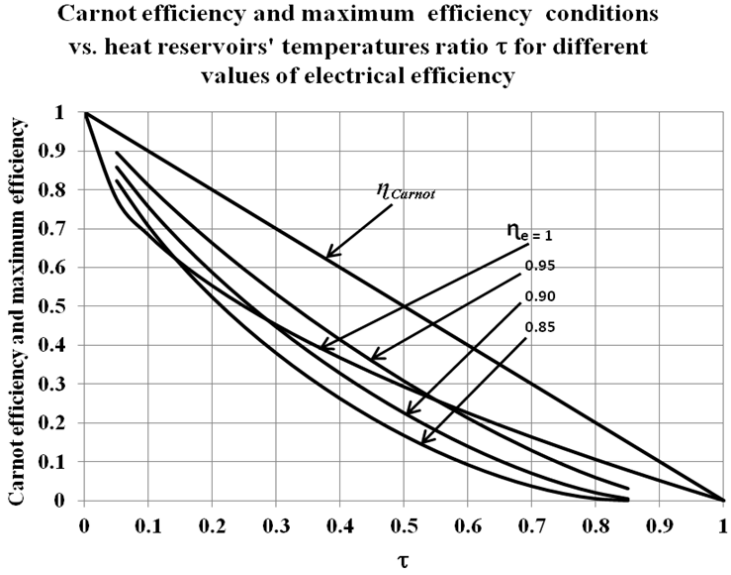

Fig. 13 Maximum efficiency point plotted as a function of the variable τ and the electrical efficiency parameter

2. Effects of Isentropic Efficiency

The following values were used for isentropic efficiency—1.0, 0.95, 0.9, and 0.85.

As can be seen from Fig. 14, the maximum efficiency point is reduced below the case of Carnot efficiency.

3. Effect of Heat Leak

The following values were used for the dimensionless heat leak parameter —0.0, 0.05, 0.1, and 0.15.

As can be seen from Fig. 15, the maximum efficiency point is reduced below the case of Carnot efficiency.

4. Combined Effect of the Dissipation Mechanisms

The following values of the dissipation parameters were used as was described in the numerical section. Three value sequences were used for dissipation as follows: 1.0, 1.0, 0.0 for ideal case; the values are given for electrical efficiency and isentropic efficiency and dimensionless heat leakage coefficient in order. The other sequence values are: 0.95, 0.95, 0.05; 0.9, 0.9, 1.0; and 0.85, 0.85, 0.15. 9 were used.

As can be seen from Fig. 16, the maximum efficiency point is reduced below the case of Carnot efficiency. Even a 1% change in the combined effect leads to a substantial change in maximum efficiency.

V. Discussion

The power-efficiency curves were produced for the MHD power generator in a manner similar to that done for different heat engine types and different dissipation mechanisms [8], [9]. It is found that the constant velocity condition of the working fluid in the MHD generator of the MHD system leads to qualitatively similar behavior of the power-efficiency curves as frictional losses in the compressor modeled via the isentropic efficiency and as the effect of the heat leak from the hot side to the cold side. For the non-ideal case, both maximum efficiency and efficiency at the maximum power point operation vanish at the extremes of both slow operation

and fast operation.

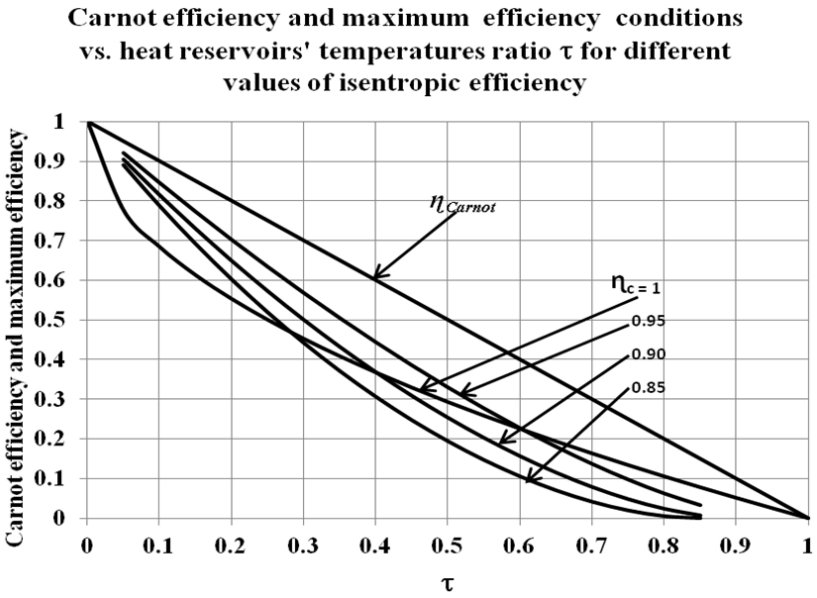

Fig. 14 Maximum efficiency point plotted as a function of the variable τ and the isentropic efficiency parameter

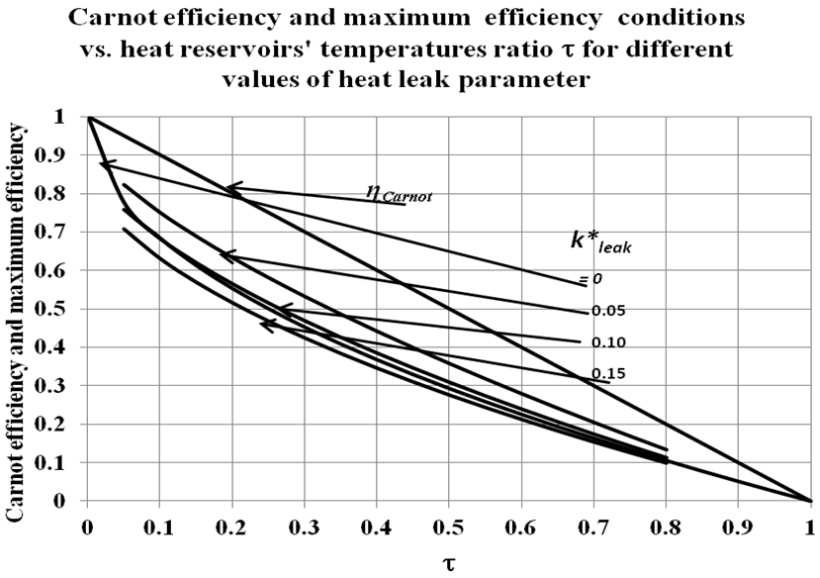

Fig. 15 Maximum efficiency point plotted as a function of the variable τ and the dimensionless heat leak parameter

For the ideal case, when the value of the electrical efficiency is 1.0, the value of the isentropic efficiency is 1.0, and there is no heat leak, the efficiency at maximum power operation approaches the Curzon & Ahlborn efficiency [11], [12] and the maximum efficiency approaches the Carnot efficiency [12].

VI. Summary and Conclusions

The MHD system is approximated by a gas turbine model (Brayton-MHD model) and analyzed with the following dissipation mechanisms: constant velocity of the working fluid in the MHD generator, frictional losses in the compressor, and heat leakage from the hot side to the cold side. The performance of the MHD generator is modeled by the electrical efficiency that was defined by (5). The frictional losses in the compressor are modeled via the isentropic efficiency of the compressor; the heat leak is proportional to the temperature difference between the temperature of the hot heat reservoir and the temperature of the cold heat reservoir.

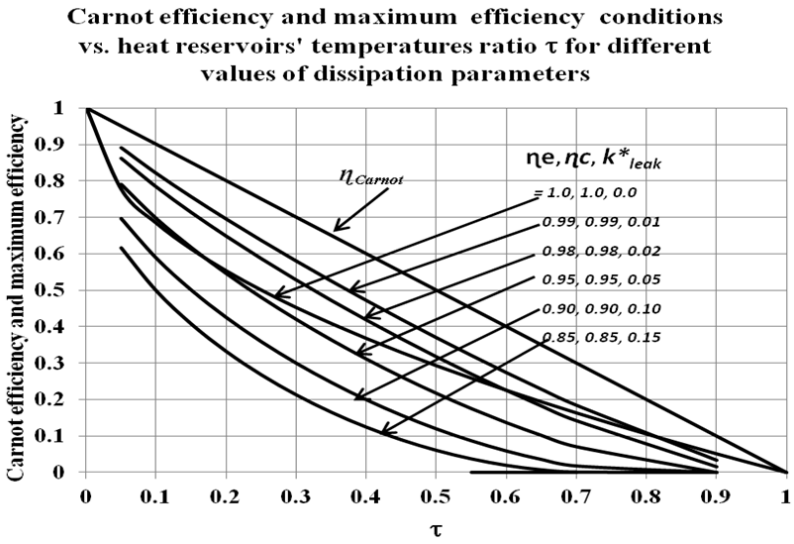

Fig. 16 Maximum efficiency point plotted as a function of the variable τ and the combined effect of dissipation parameters

The characteristics of the MHD system were presented by means of the power-efficiency curves, with different dissipation parameters as were described in IV. The power efficiency plots demonstrated the general loop shape and qualitatively, the same behaviors were observed. The locus of the maximum power point operation and the locus of the maximum efficiency were added to the plots for explicit demonstration.

The maximum power point operation was derived analytically and the maximum efficiency was determined numerically by means of the GOALSEEK tool of the Microsoft Excel program.

It was observed that the efficiency at maximum power operation and the maximal efficiency are very sensitive to the dissipation parameters. In order to improve their values, special care and engineering design is needed.

References

[1] Ajith Krishnan, R. and Jinshah, B.S. (2013): Magnetohydrodynamic Power Generation, IJSRP. 3(6): 1-11.
[2] Sutton, G. W. (1962): The theory of magnetohydrodynamic power generators, Armed Services Technical Information Agency. Accession No. 296430: 1-215.
[3] Sheindlin, A. E., et al. (1979): Magneto hydrodynamic power generation, Nat. Resour. Forum. 3(2):133-145.
[4] Brogan, T. R. (1964): MHD power generation. IEEE Spectr. 1(2): 58-65.
[5] El Haj Assad, M. (2015): Thermodynamic Analysis of MHD Power Cycle, J Robot Mech Eng Resr 1(1).
[6] Fung; T. K., et al. (1980): An Alternate Approach to the Application of MHD Power Generation Technology in a Utility Environment. IEEE Transactions on Power Apparatus and Systems., PAS-99(3): 1306-1312.
[7] Smith, J. L. (1984): Magnetohydrodynamic Power Generation. NASA Technical Report NASA-TP-2331, NAS 1.60:2331. 1-31.
[8] Gordon, J.M/ and Huleihil, M. (1991): On optimizing maximum-power heat engines. J. Appl. Phys., 69(1): 1–7.
[9] Gordon, J.M. and Huleihil, M. (1992): General performance characteristics of real heat engines. J. Appl. Phys., 72(3): 829–837.
[10] Spring, K. H. (ed.) (1965). Direct generation of electricity. London; New York: Academic Press.
[11] Curzon, F.L. and Ahlborn, B. (1975): Efficiency of a Carnot engine at maximum power output. Am. J. Phys. 43(1): 22–24.
[12] Leff, H. S (1987): Thermal efficiency at maximum work output: New results for old heat engines. Am. J. Phys. 55(7): 603-610.